

Noncontact friction force microscopy based on quartz tuning fork sensors

M. Labardi^{a)} and M. Allegrini^{b)}

PolyLab-CNR and Dipartimento di Fisica, Università di Pisa, Largo Bruno Pontecorvo 3, I-56127 Pisa, Italy

(Received 15 June 2006; accepted 18 September 2006; published online 25 October 2006)

Noncontact friction force microscopy (NC-FFM) measures the damping of the resonant oscillation of an atomic force microscope (AFM) tip that vibrates parallel to the sample surface at a controlled distance. By exploiting the two fundamental orthogonal vibration modes of a quartz tuning fork, such technique can be realized by all-piezoelectric sensing by simultaneously employing an AFM noncontact mode for distance control. The low noncontact-mode vibration amplitude used increases the effective interaction time for shear measurement. Application to polymeric samples shows that the dissipation contrast of NC-FFM is higher than that of the corresponding noncontact-mode phase imaging. © 2006 American Institute of Physics. [DOI: 10.1063/1.2369637]

Friction force microscopy (FFM) was conceived, in analogy to macroscopic sliding friction measurements, to discriminate materials on a surface by virtue of their frictional properties on the microscopic and nanoscopic scales. This is customarily done by using the stylus of an atomic force microscope (AFM) dragged over the surface while being pushed against it with controlled load. Accurate control of forces and displacements in atomic-resolution AFM has provided strong insight into nanoscale dissipative processes, giving birth to the field of nanotribology.¹ The bidirectional AFM based on optical lever detection² has provided a convenient means to simultaneously detect both loading force (measured by cantilever bending) and frictional force (given by cantilever twisting), helping us to extend nanotribology in materials science and engineering as well as to numerous applications, for instance, magnetic data storage.¹

When the probe tip could not be applied on a cantilever structure, like in the case of early fiber-based scanning near-field optical microscopy (SNOM), the tip was oscillated at resonance and parallel to the surface, and damping of such oscillation, mainly related to energy dissipation, was exploited for probe/sample distance control, realizing shear-force microscopy.^{3,4} The physical processes involved in such measurement are still under debate;⁵ therefore studies aimed at independent measurements of conservative and dissipative contributions causing oscillation amplitude changes in shear-force microscopy are in order. Similar interpretative issues concern the AFM noncontact-mode technique, and more generally dynamic force microscopy,⁶ in which influence of both conservative and dissipative interactions is present as well.⁷ Simultaneous normal and shear interaction measurements is feasible by using AFM cantilevers excited at both bending and twisting resonances.^{8,9} The measurement of damping of the resonant oscillation of an AFM tip that vibrates parallel to the sample surface, with controlled average distance in the noncontact AFM regime (1–10 nm), is named noncontact FFM (NC-FFM).⁹

Experimental activity aimed to study, for instance, the issue of single-atom friction processes^{10,11} and quantum friction¹² needs implementation of atomic and friction force

microscopies in ultrahigh vacuum (UHV) and/or cryogenic environment, where standard optical lever or interferometric detection systems may suffer from misalignments due to mechanical and thermal drifts into the vacuum chamber. Furthermore, the laser beam employed to detect the probe displacement causes heating of the cantilever and increases thermal noise.¹³ Therefore, more practical and inexpensive measurement setups are demanded.

An example of such kind of simplification is represented by the use of quartz tuning forks as self-sensing, compact, inexpensive, and accurate force sensors. Their operation in UHV or cryogenic environments is convenient due to their stand-alone performance, needing no optical detection systems.¹⁴ Atomic resolution in frequency-modulation AFM as well as shear-force microscopy has been demonstrated by means of such sensors.^{10,15} Tuning forks were introduced as shear-force sensors for fiber-optic SNOM (Ref. 16) and now represent the most widely used detection system for such microscopes. They also demonstrated their unique performances for atomically resolved dynamic-force microscopy^{6,17} as well as for atomic-scale friction measurements.¹⁰ In this letter, we report on the use of such sensors for the measurement of friction forces while simultaneously sensing the probe/sample distance in the usual AFM noncontact mode, realizing thereby NC-FFM based on nonoptical, compact sensing of both normal and lateral interactions.

Briefly, the tuning fork is a quartz oscillator shaped to have a well-defined resonance frequency and a high Q factor, and provided with metal electrodes that pickup the piezoelectric charge caused by the crystal deformation. A sketch of the geometry of a tuning fork is shown in Fig. 1. The bending vibration mode at the nominal resonance frequency f_z is antisymmetric along z ; i.e., the two prongs vibrate in phase opposition. Such mode is only affected by internal dissipation in the fork material, since the center of mass is conserved and energy dissipation through the fork base is minimal. Therefore, typical Q factors in air are of the order of 10^3 – 10^4 .

Tuning fork prongs have a typical width over thickness ratio of about 1/2. In this they differ strongly from usual AFM cantilevers, for which the thickness is far smaller than both width and length. This implies the existence of another bending vibration mode, orthogonal to the one exploited for

^{a)}Electronic mail: labardi@df.unipi.it

^{b)}Present address: Physics Laboratory, National Institute of Standards and Technology, Gaithersburg, MD 20899.

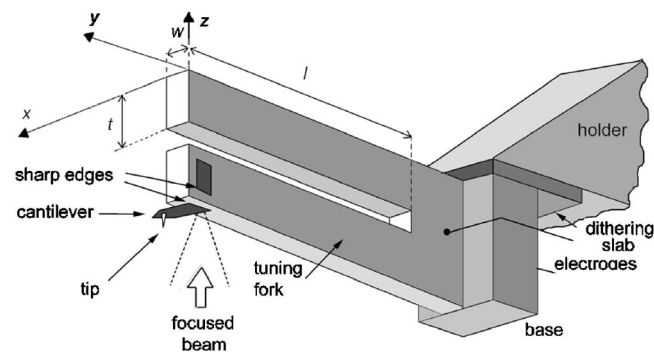


FIG. 1. Sketch of the tuning fork/AFM tip mount geometry and of the optical detection system used for displacement calibration.

the usual quartz operation, with about half its resonance frequency, that we refer to as the x mode. The electrode configuration of tuning forks is not the most favorable for the detection of such x mode, since it is optimized to detect the z mode.¹⁸ However, we have observed that such resonance shows up in the tuning fork piezoelectric response spectrum as a function of vibration frequency. In Figs. 2(a) and 2(b) we show the piezoresponse spectrum of a common tuning fork (nominal parameters: $f_N=32\,768$ Hz, prong length $l \approx 4.0$ mm, width $w \approx 0.3$ mm, and thickness $t \approx 0.6$ mm). The fork is mechanically excited by means of a piezoactuator vibrating along the z axis. The vibration amplitude spectrum is measured by sending the preamplified ($500\times$) output voltage of the tuning fork to a lock-in amplifier and by sweeping the excitation frequency. We have found that the mode at frequency f_x [Fig. 2(a)] is detected with about 12 times less sensitivity than the one at f_z [Fig. 2(b)].

The vibration modes have been identified in this work by direct measurement of displacements in both x and z directions by means of an optical detection method. The reflection of a focused laser beam has been used to detect displacements in a single direction, with negligible influence by displacements in the orthogonal direction, as directly checked. The laser beam is focused on the edge of an AFM cantilever, that we glued to the tuning fork prong. The chosen edge is sharp and perpendicular to the movement to be detected (as sketched in Fig. 1). The reflection signal is detected by a photomultiplier and sent to a lock-in amplifier as previously

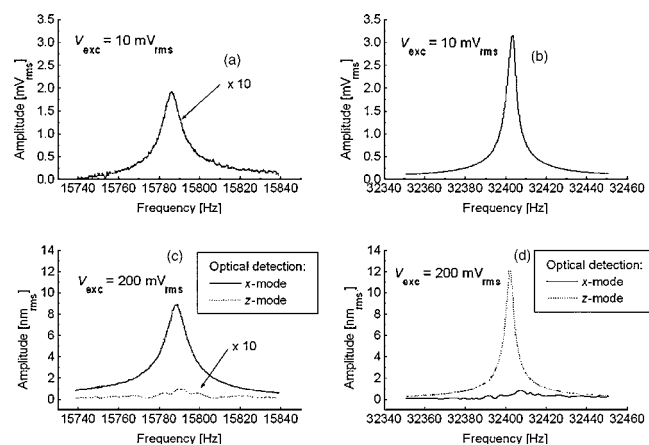


FIG. 2. (a), (b) Piezoresponse spectrum of a common tuning fork around the resonance frequency of the x and z modes. (c), (d) Optically detected resonance spectra of a quartz tuning fork in orthogonal directions. Solid line: x direction; dotted line: z direction.

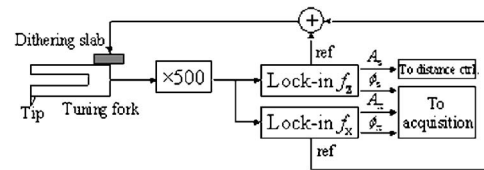


FIG. 3. Sketch of the tuning fork setup for AFM application.

described. Two cantilever segments have been glued onto orthogonal sides of the same prong in order to allow measurement of displacements along both x and z directions.

The vibration spectra along the two directions, as determined optically, are shown in Figs. 2(c) and 2(d). The modes at frequency f_x and f_z are clearly orthogonal. The x mode (at $f_x=15\,788$ Hz in this case) presents comparable oscillation amplitude with respect to the z mode, although one would expect the z motion to be excited more efficiently, since the excitation motion is along the z direction. The piezoelectric coefficient for the x -direction motion results in $C_x=2.23\ \mu\text{V}/\text{nm}$, while the for the z direction is $C_z=27\ \mu\text{V}/\text{nm}$ (nominal). It is evident that the obtained piezoelectric signal for the x mode is high enough for reliable use as a dynamic force microscopy sensor. Furthermore, the quality factor of such resonance is pretty high, even though smaller than that of the z mode at f_z . This also suggests that the x mode is antisymmetric, like the z mode. The Q factors obtained by direct optical measurement of the displacements are similar to those carried out by the piezoresponse spectra (4814 vs 4410, respectively, for the z mode, and 994 vs 1138 for the x mode).

The described sensor has been applied for AFM imaging as shown in Fig. 3. The oscillation mode of the tip consists of two simultaneous vibrations, excited at the two different resonant frequencies f_z and f_x . The two resonant motions will occur perpendicularly to each other, one along z (normal) and the other along x (lateral). AFM distance control is performed in the noncontact mode by stabilizing the amplitude of the normal oscillation A_z , measured by a dual-phase lock-in amplifier referenced at f_z , while the normal phase ϕ_z provides the “phase imaging” information. The lateral vibration amplitude A_x and phase ϕ_x , measured by a second dual-phase lock-in amplifier referenced at f_x , provide instead an independent measurement of shear dissipation. Compared to previous experiments, here we adopt the tuning fork sensor instead of the special⁸ or standard cantilevers.^{9,19}

For the purpose of increasing the imaging speed in the noncontact mode, our tuning fork was modified in order to lower the Q factor of the z -mode oscillation.²⁰ Glue was spread on the fork prong not holding the AFM tip in such a way to immobilize preferentially its z motion. In this way, we have obtained a Q factor of about 600 for the z mode, while still maintaining a Q factor of about 300 for the x mode. Such values allow good sensitivity while enabling faster scan rates in the noncontact mode. Use of the frequency-modulation detection scheme²¹ should allow faster scanning also with higher- Q tuning forks.

The experimental setup is comprised of a scanning probe microscope (SPM) controller (SPM1000, RHK Technology, USA) interfaced to a home-built, tuning-fork-based AFM head, equipped with a linearized sample scan stage (517.3CL, Physik Instrumente, Germany), and operated in air.

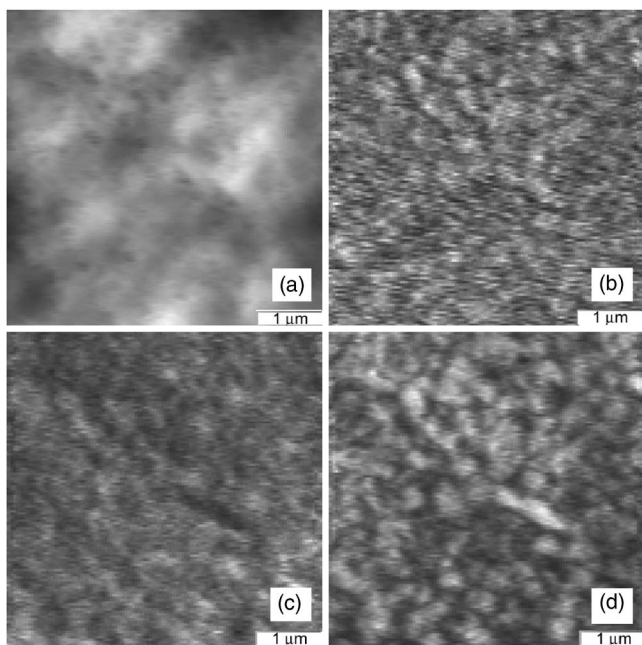


FIG. 4. (a) Topography and (b) noncontact-mode phase image of a polyethylene film. (c) Lateral vibration amplitude and (d) phase recorded simultaneously. All images are raw data.

The performance of NC-FFM was tested on a low-density polyethylene film (Fig. 4). The used free oscillation amplitudes were $0.9 \text{ nm}_{\text{rms}}$ for the noncontact mode and $2 \text{ nm}_{\text{rms}}$ for lateral oscillation. Stabilization in the repulsive noncontact regime was necessary to obtain the best image contrast; operation in the attractive noncontact regime as well as in the indentation regime, where the average interaction force was too high and damaged the polymer surface, provided poor image contrast. In repulsive noncontact mode, the sample surface was not modified by the scan, as verified by a comparison of trace and retrace scans as well as by a comparison of repeated scans. Performance of approach curves show that in the attractive regime of noncontact mode, lateral amplitude has small or no decrease, while after the transition to the repulsive regime, a strong drop of lateral amplitude is observed. The images reported in Fig. 4 were obtained in the repulsive regime, with a normal amplitude of $0.8 \text{ nm}_{\text{rms}}$ and a lateral amplitude of the order of $0.7 \text{ nm}_{\text{rms}}$. It is evident from Fig. 4 that the lateral amplitude and especially phase images provided higher contrast with respect to the usual noncontact-mode phase imaging and that information contained therein differs from the one of both topography and noncontact mode phase. Test measurements made on stiffer samples (not shown) lead to higher resemblance between normal and lateral phase images. It may be speculated that in the case of the stiffer samples, the main effect on the lateral channel is the conservative interaction, where the local surface slope has a main role,^{5,10,11} while for compliant samples, such as the polymeric one reported here, shear dissipation prevails over the conservative interaction.

The influence of topography in dissipation measurement is one concern of this study. Its role could be completely ruled out only by a distance stabilization method not sensitive to dissipation at all, obtainable, for instance, with the frequency-modulation detection scheme under special condi-

tions, namely, exact 90° self-oscillator phase.⁷ Furthermore, since different dissipation mechanisms could be related to normal and lateral tip motions, independent images of “normal” and “lateral” dissipations would be needed to discriminate between them.

A further remarkable advantage of the present technique compared to the ones based on standard cantilevers is that AFM dynamic modes can be performed here at very low amplitudes (below 1 nm) while avoiding snap to contact. This reduces the average tip/sample distance compared to cantilevers and therefore increases the effective tip/sample interaction time, leading to higher shear dissipation.

In conclusion, a practical and inexpensive piezoelectric sensor for noncontact friction force microscopy has been developed based on common quartz tuning forks. Employment of this sensor might be particularly useful in UHV and/or cryogenic environment, where optical detection is difficult to implement. We believe that the use of the reported sensor in combination with frequency modulation detection is promising for the study of surface dissipation mechanisms by AFM and especially for the characterization and differentiation of normal and shear friction processes.

Financial support from Italian MIUR through the PRIN project “Nanotribology” and from Fondazione Cassa di Risparmio di Pisa is acknowledged.

¹B. Bhushan, *Principles and Applications of Tribology* (Wiley, New York, 1999).

²G. Meyer and N. M. Amer, *Appl. Phys. Lett.* **57**, 2089 (1990).

³P. C. Yang, Y. Chen, and M. Vaez-Iravani, *J. Appl. Phys.* **71**, 2499 (1992).

⁴E. Betzig, J. K. Trautman, R. Wolfe, E. M. Gyorgy, P. L. Finn, M. H. Kryder, and C. H. Yang, *Appl. Phys. Lett.* **61**, 142 (1992).

⁵M. J. Gregor, P. G. Blome, J. Schöfer, and R. G. Ulbrich, *Appl. Phys. Lett.* **68**, 307 (1996); M. A. Drummond Roby, G. C. Wetsel, Jr., and C.-Y. Wang, *ibid.* **69**, 130 (1996); R. D. Grober, J. Acimovic, J. C. Schuck, D. Hessman, P. J. Kindlemann, K. Karrai, I. Tiemann, and S. Manus, *Rev. Sci. Instrum.* **71**, 2776 (2000).

⁶F. J. Giessibl, *Science* **267**, 68 (1995).

⁷B. Gotsmann, C. Seidel, B. Anczykowski, and H. Fuchs, *Phys. Rev. B* **60**, 11051 (1999).

⁸S. P. Jarvis, H. Yamada, K. Kobayashi, A. Toda, and H. Tokumoto, *Appl. Surf. Sci.* **157**, 314 (2000).

⁹Proceedings of the Second World Tribology Congress, Wien, Austria, 3–7 September 2001 (unpublished) (see <http://www.oetg.at/website/wtc2001cd/html/M-81-01-901-labardi.pdf>).

¹⁰F. J. Giessibl, M. Herz, and J. Mannhart, *Proc. Natl. Acad. Sci. U.S.A.* **99**, 12006 (2002).

¹¹S. Kawai, S. Kitamura, D. Kobayashi, and H. Kawakatsu, *Appl. Phys. Lett.* **87**, 173105 (2005).

¹²J. B. Pendry, *J. Phys.: Condens. Matter* **9**, 10301 (1997).

¹³M. Allegrini, C. Ascoli, P. Baschieri, F. Dinelli, C. Frediani, A. Lio, and T. Mariani, *Ultramicroscopy* **42–44**, 371 (1992).

¹⁴S. Hembacher, F. J. Giessibl, and J. Mannhart, *Appl. Surf. Sci.* **188**, 445 (2002).

¹⁵F. J. Giessibl, *Appl. Phys. Lett.* **76**, 1470 (2000).

¹⁶K. Karrai and R. D. Grober, *Appl. Phys. Lett.* **66**, 1842 (1995).

¹⁷W. H. J. Rensen, N. F. van Hulst, A. G. T. Ruiter, and P. E. West, *Appl. Phys. Lett.* **75**, 1640 (1999).

¹⁸J. F. Nye, *Physical Properties of Crystals* (Oxford, London, 1957).

¹⁹T. Kunstmann, A. Schlarb, M. Fendrich, D. Paulkowski, Th. Wagner, and R. Möller, *Appl. Phys. Lett.* **88**, 153112 (2006).

²⁰The used method is similar to the one used by F. J. Giessibl, *Appl. Phys. Lett.* **73**, 3956 (1998).

²¹T. R. Albrecht, P. Grütter, D. Horne, and D. Rugar, *J. Appl. Phys.* **69**, 668 (1991).